

Enhanced absorptance of gold following multipulse femtosecond laser ablation

A. Y. Vorobyev and Chunlei Guo

The Institute of Optics, University of Rochester, Rochester, New York 14627, USA

(Received 28 April 2005; revised manuscript received 2 September 2005; published 21 November 2005)

In contrast to the common belief for femtosecond laser ablation that the thermal energy remaining in the ablated sample should be negligible, we recently found that a significant amount of residual thermal energy is deposited in metal samples following multishot femtosecond laser ablation. This suggests that there might be a significant enhancement in laser light absorption following ablation. To understand the physical mechanisms of laser energy absorption, we perform a direct measurement of the change in absorptance of gold due to structural modification following multishot femtosecond laser ablation. We show that besides the known mechanisms of absorption enhancement via microstructuring and macrostructuring, there is also a significant absorption enhancement due to nanostructuring. It is found that nanostructuring alone can enhance the absorptance by a factor of about three. The physical mechanism of the total enhanced absorption is due to a combined effect of nanostructural, microstructural, and macrostructural surface modifications induced by femtosecond laser ablation. Virtually, at a sufficiently high fluence and with a large number of applied pulses, the absorptance of gold surface can reach a value close to 100%.

DOI: [10.1103/PhysRevB.72.195422](https://doi.org/10.1103/PhysRevB.72.195422)

PACS number(s): 68.47.De, 68.35.-p, 79.20.Ds, 68.37.Hk

I. INTRODUCTION

Recently, much research activity has been focused on both physical processes of femtosecond laser ablation¹⁻³ and its applications for high-precision materials micromachining,⁴ thin-film deposition,⁵ generation of ultrashort x-ray pulses,⁶ and synthesis of nanoparticles.⁷⁻⁹ It is commonly believed that one of the most important advantages of femtosecond laser ablation is that the energy deposited by ultrashort laser pulses does not have enough time to move into the bulk sample. Therefore, the residual thermal energy remaining in the bulk sample should be negligible. Recently, we performed a direct measurement on the thermal energy remaining in bulk metals following multipulse femtosecond laser ablation. In contrast to the previous belief, we found a significant amount of residual thermal energy deposited in various metals.¹⁰ We suspect that an enhancement in absorption following femtosecond laser ablation is an important factor contributing to the enhanced residual thermal energy. However, it is unclear how a femtosecond laser will induce such a noticeable change in absorption.

The absorptance A of a pure metal with a clean surface consists of two components¹¹⁻¹³

$$A = A_{INTR} + A_{SR},$$

where A_{INTR} is the intrinsic absorptance and A_{SR} is the contribution due to surface roughness. For an optically smooth metal surface, A_{SR} is about 1–2% of A_{INTR} ¹³ but the role of A_{SR} enhances as the surface roughness increases. For multipulse ablation, only the first femtosecond laser pulse interacts with an undamaged surface, since the laser-induced surface structural modification develops long after the ultrashort pulse. In this case, A is governed by A_{INTR} , which can be a function of laser fluence due to laser-induced change in the dielectric constant of the material. All the subsequent laser pulses interact with a structurally modified surface and their absorption is determined by both A_{INTR} and A_{SR} . The absorp-

tion of a single femtosecond laser pulse by an undamaged metal surface has been studied in the past, where the absorption is dominated by A_{INTR} .¹⁴⁻¹⁷ However, the coupling of laser energy to a metal in multipulse femtosecond laser ablation has not yet been investigated, where A_{SR} may have a significant value due to surface structural modification.

In this paper, we study the effect of surface structural modifications on the absorptance of gold in multipulse femtosecond laser ablation when an originally plane and smooth surface transforms into a blind hole. This effect is investigated as a function of the number of applied ablation pulses at various fluences. To study the absorptance, we apply a laser calorimetry technique,^{10,12} allowing a direct measurement of laser energy absorbed by the sample. We show that femtosecond laser-induced surface modification enhances the sample absorptance that can reach a value close to 100% at a sufficiently high fluence with a large enough number of applied pulses. To understand the physical mechanism of this large enhancement in energy absorption, we also examine the surface modifications using a scanning electron microscope (SEM). We show that besides the known mechanisms of absorption increase via microstructuring and macrostructuring, there is also a significant absorption enhancement due to nanostructuring. It is found that nanostructuring alone can enhance the absorptance by a factor of about 3.

II. EXPERIMENTAL SETUP

In our experiment, we use an amplified Ti:sapphire system generating 60-fs pulses of about 1.5 mJ/pulse at 1-kHz repetition rate and with a central wavelength at 800 nm. The laser beam is focused onto a sample with a 40-cm-focal-length lens at normal incidence. An electromechanical shutter is used to select the number of pulses, N , applied to the sample. The absorptance of the ablated spot is studied in the following way. After ablation of the sample with a chosen number of pulses, we reduce the laser fluence

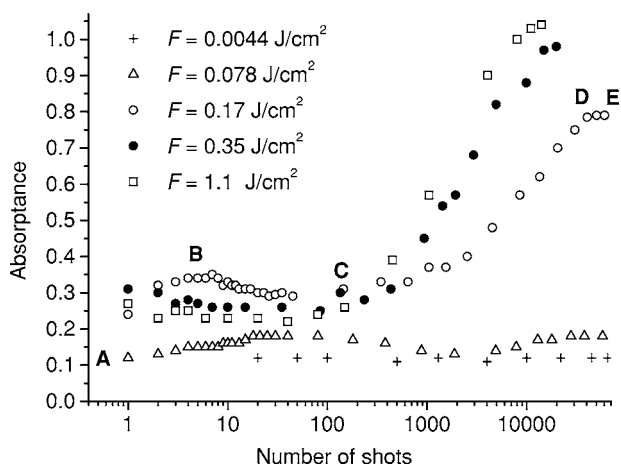


FIG. 1. Absorbance of gold surface following femtosecond laser ablation as a function of the number of pulses at various F . The measured absorbance is slightly higher than 1 at $F=1.1$ J/cm² due to the 10% measurement uncertainty discussed in the text.

to a level much below the ablation threshold. Subsequently, we irradiate the ablated spot again using a train of low-fluence laser pulses that will not induce any further surface modification. A certain amount of energy from this low-fluence pulse train, E_A , is absorbed in the skin layer of the sample, dissipates via heat conduction in the sample, and causes its bulk temperature rise, ΔT . We measure this temperature rise with a thermocouple battery that allows E_A to be determined calorimetrically as $E_A = C\Delta T$, where C is the known heat capacity of the sample. The details of this calorimetric technique have been described elsewhere.¹⁰ The measurement error for E_A is estimated to be about 10%. To measure energy E_I incident upon the sample, a certain fraction of incident pulse train energy is split off by a beam splitter and measured with a joulemeter. The measurement error of E_I is estimated to be about 5%. Having measured E_I and E_A , the absorbance of the ablated spot can be found as $A = E_A/E_I$. Laser-induced surface modifications are studied using a SEM and an optical microscope. The sample surface is mechanically polished.

III. EXPERIMENTAL RESULTS AND DISCUSSION

The optical properties of surface modifications are studied following multipulse ablation at single-pulse laser fluences of $F=1.1$, 0.35, 0.17, and 0.078 J/cm² in air. The ablation threshold F_{abl} for a pristine surface is found to be $F_{abl}=0.067$ and 0.048 J/cm² for single-pulse and 500-pulse train irradiation, respectively. The numbers of pulses required to perforate a 1-mm-thick sample at the center of the irradiated spot are determined to be 16 100, 25 000, and 77 000 pulses at $F=1.1$, 0.35, and 0.17 J/cm², respectively. This corresponds to average ablation rates of 63, 40, and 13 nm/pulse, indicating that a single laser pulse produces a nanoscale modification in depth. Plots of absorbance versus the number of ablation shots, N , at different F are shown in Fig. 1. For an undamaged surface, we can see that the absorbance remains a constant value of 0.12 when measured at

$F=0.0043$ J/cm², which is an order of magnitude below F_{abl} . The absorbance of a structurally modified surface is significantly greater than that of the undamaged surface and shows dependence on the number of applied ablation pulses, N .

The $A(N)$ curves for the ablated surface can be characterized into four distinct regions marked with A, B, C, D, and E on $A(N)$ in the case of $F=0.17$ J/cm² in Fig. 1.

(i) Region AB, where the absorbance initially increases from 0.12 (undamaged surface) to a value in the range of 0.25–0.33. Typically, this region covers the first 1–10 shots. For example, this initial enhancement of absorbance can be produced by four pulses at $F=0.17$ J/cm² or by one pulse at $F=0.35$ and 1.1 J/cm². An optical microscopy study shows that the irradiated spot is entirely covered with surface modification following ablation by only one pulse when $F \geq 0.35$ J/cm², but by four pulses at $F=0.17$ J/cm². Therefore, the enhancement of absorbance with N at $F=0.17$ J/cm² appears due to both the surface modification and an increase in size of the modified area.

(ii) Region BC, where absorbance undergoes a slight decrease as N increases. Typically, this region covers approximately the next 100–300 pulses. Both regions AB and BC extend to a larger number of pulses when the surface is modified at F only slightly above F_{abl} , as seen from the curve at $F=0.078$ J/cm² in Fig. 1.

(iii) Region CD is characterized by a further enhancement of absorbance with the increase of N . This region extends to N of an order of 10 000 pulses.

(iv) Region DE, where absorbance reaches the maximum value that does not change with further increase of N .

In order to understand how surface modifications affect absorbance, we take the SEM pictures of surface morphology shown in Figs. 2–6. In AB, BC, and CD regions, where absorbance exhibits dependence on N , the following surface modifications are typically observed. For region AB, a characteristic modification is nanoscale roughness (Fig. 2). In region BC, two major features are observed. First, nanoscale roughness develops further in the form of nanobranches [Fig. 3(a)] and spherical nanoparticles [Fig. 3(b)]. Secondly, microscale structures begin to develop in the forms of micropores, circular microgrooves, and central microchannels. In region CD, we start to observe features like a crater with a deep central microchannel, periodic structures with orientation in the direction perpendicular to the laser light polarization and with a period roughly equal to the laser wavelength [Fig. 4(a)], and a visible black halo around the crater. All these laser-induced surface modifications can affect the absorbance in various ways. Surface roughness^{12,18} can enhance the absorption of light both by multiple reflections in microcavities and by variation in the angle of incidence (angular dependence of Fresnel absorption). Nanoscale structural features can affect absorbance since the optical properties of a nanostructured material can be quite different from the bulk.^{19,20} Laser-induced periodic surface structures (LIPSS) may enhance absorption of laser energy via generation of surface electromagnetic waves.^{13,21} It is worthy to mention that the LIPSS observed in our experiment has even finer nanoscale structural features shown in Fig. 4(b).

Our study shows that the absorption of laser energy in femtosecond laser ablation can also be altered through rede-

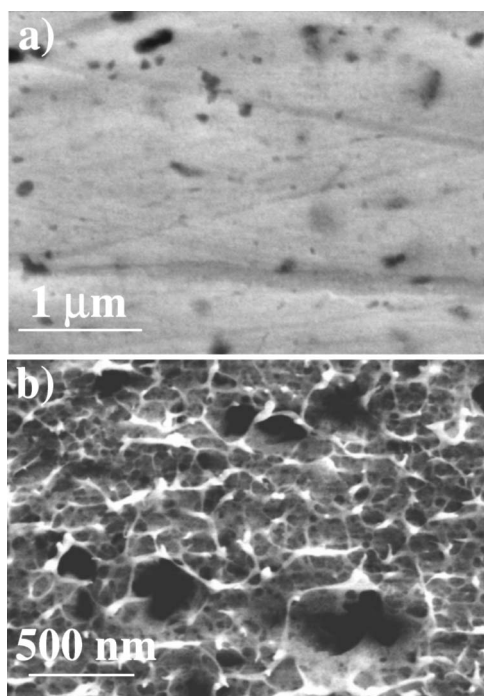


FIG. 2. SEM images of the Au surface (a) before irradiation and (b) after 1 shot at $F=1.1 \text{ J/cm}^2$. This nanoscale roughness produced by ablation enhances the absorptance by a factor of 2 (region AB in Fig. 1).

position of ablated material. The examination of the black halo produced around the crater shows that its elemental composition determined by energy dispersive x-ray analysis

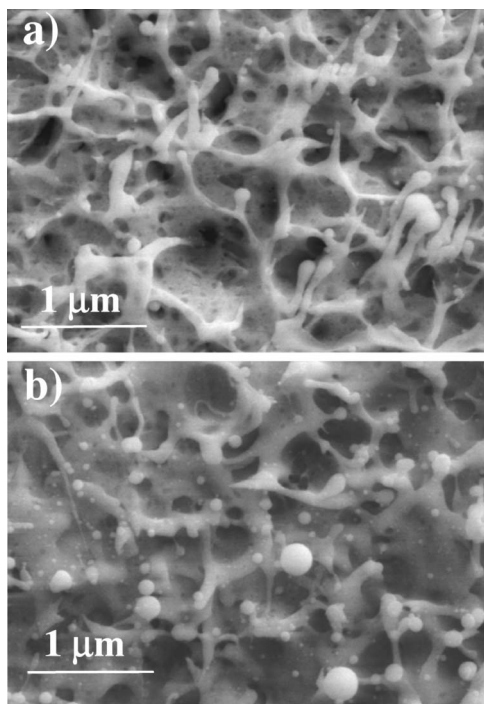


FIG. 3. Nanoscale surface structural features produced at $F=1.1 \text{ J/cm}^2$ (region BC). (a) Nanobranches after two-shot ablation. (b) Spherical nanoparticles after five-shot ablation.

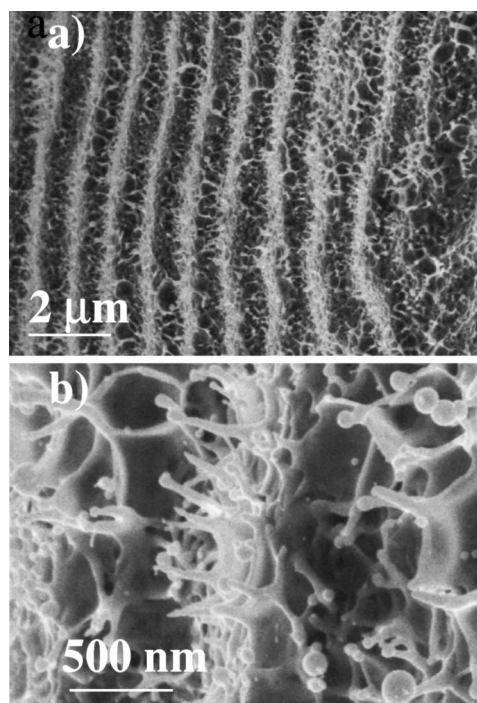


FIG. 4. LIPSS produced in irradiated area by 20 000 shots at $F=0.17 \text{ J/cm}^2$ (region CD in Fig. 1). (a) SEM micrograph showing the period of LIPSS. (b) Nanobranches and supported spherical nanoparticles in LIPSS.

is identical to that for a pristine surface, i.e., the black halo is a layer of the ablated and redeposited gold. SEM images in Figs. 5 and 6 demonstrate that the black halo has a structure of spherical nanoparticle aggregates that is typically seen in gold-black films.^{22,23} The gold-black films have been known for their high absorptance in the infrared.^{24,25} Therefore, the gold-black halo can enhance the absorption of low-intensity wings of the incident Gaussian beam and contribute to residual heating of the sample.¹⁰ Since redeposition of ablated material occurs both outside and within the ablated spot, the redeposition of the nanoparticles produced by ablation can also enhance the absorption of light in the ablated area. For example, an enhanced absorption of light by a semiconductor coated with Au nanoparticles has recently been reported.²⁶ Therefore, in femtosecond laser ablation, the enhanced absorption can occur due to surface nanostructures, microstructures, macrostructures, and redeposition of nanoparticles depending on ablation conditions. The combined effect of these surface modifications can lead to virtually 100% absorption of laser light in multipulse ablation with a sufficiently large number of pulses at high fluence as shown in Fig. 1. Previously,¹⁰ we have also found that, under the same ablation conditions, almost all incident laser energy is retained in the sample as the residual thermal energy. This suggests that the energy carried away by the ablated material is small in Au, and the enhanced absorptance observed here appears to be the dominant factor in the enhanced residual thermal energy deposition observed previously⁵ in multipulse femtosecond laser ablation at large numbers of applied pulses.

Since different surface modifications are superimposed on each other, it is difficult to completely isolate and determine

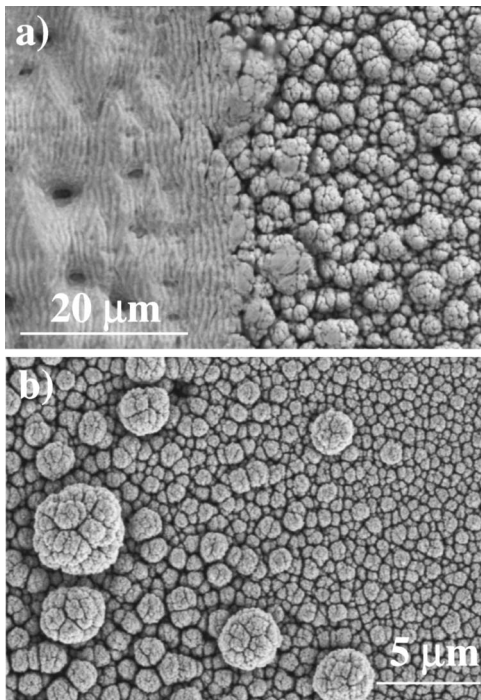


FIG. 5. (a) LIPSS on the periphery of irradiated area and gold-black deposit outside the irradiated area after 10 000 shots at $F=1.1 \text{ J/cm}^2$ (region *DE*). (b) Gold-black deposit after 20 000 shots at $F=0.17 \text{ J/cm}^2$ (region *CD* in Fig. 1). Gold-black layer consists of spherical aggregates. Their mean diameter decreases as the distance from the crater increases. A spherical aggregate consists of spherical nanoparticles (see Fig. 6).

each individual contribution to the enhanced absorptance. Therefore, we only provide the following estimations on the contributions of nanostructures, microstructures, and macrostructures induced by femtosecond laser ablation. Since surface nanostructures are the dominant feature in region *AB* and part of region *BC* for $N < 50-100$ and the absorptance increases from 0.12 to 0.25–0.33 over these regions (see Fig. 1), nanostructures alone account for the additional absorptance increase of about 0.1–0.2. The contribution of two types microscale structures, LIPSS and random roughness, is estimated as follows. To estimate the contribution of LIPSS, we ablate a sample using *p*-polarized light and measure the low-fluence absorptance $A(N)$ of the ablated spot with both *p*

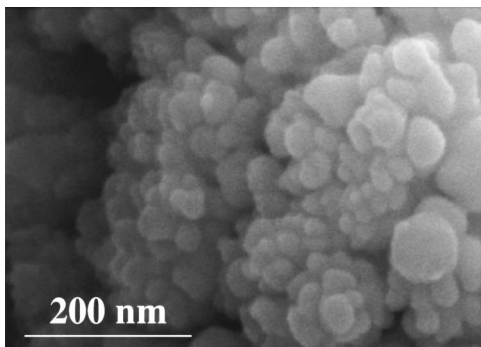


FIG. 6. SEM image of spherical nanoparticles in a spherical aggregate of the gold-black deposit.

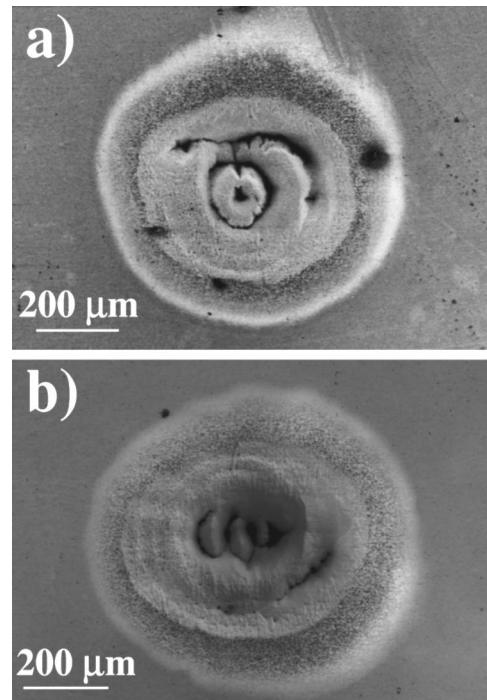


FIG. 7. (a) SEM image of a crater produced by 5000 shots at $F=0.17 \text{ J/cm}^2$; the absorptance of this ablated spot is 0.45. (b) SEM image of a crater produced by 5000 shots at $F=1.1 \text{ J/cm}^2$; the absorptance of this ablated spot is 0.85.

and *s* polarizations. The curves $A(N)$ of different polarizations are found to be identical, and this indicates that the grating effects of microscale LIPSS on the absorption of laser light is negligible. To estimate the contribution of microscale random roughness, we abrade a mechanically polished sample surface with a sandpaper to produce a rms roughness of $3 \mu\text{m}$, which is estimated to be comparable to the laser-induced roughness for $100 < N < 1000$. The absorptance of this abraded surface is then measured to be about 0.24 as opposed to 0.12 for a mechanically polished surface, and this indirectly shows that the random microroughness accounts for the additional absorptance increase of about 0.12. Macrostructures come into play in two major forms, deep central channel and concentric ring grooves, when the number of pulses is roughly larger, 500–1000, and laser fluence is higher than 0.17 J/cm^2 . Two typical SEM pictures showing macrostructure of craters are given in Fig. 7. The macroscale crater formation starts in region *CD*, and therefore, we believe the progressive increase of macrostructure size largely accounts for the absorptance increase from 0.4 to about 1.0. However, nanostructures and microstructures also develop further in regions *CD* and *DE* and may also contribute to absorptance increase to some extent.

IV. CONCLUSION

In summary, our study shows a significant increase in absorptance of gold due to surface modifications following multipulse femtosecond laser ablation. At sufficiently high fluence and with a large number of applied pulses, the ab-

sorptance can reach virtually 100%. We show that the physical mechanism of the enhanced absorption is due to a combined effect of nanostructural, microstructural, and macrostructural surface modifications induced by femtosecond laser ablation. Besides the physical mechanisms of the enhanced absorption discussed in this paper, our study also contributes to the fundamental understanding of femtosecond laser-matter interactions from the following aspects. First, laser-induced nanostructures alone can enhance the absorptance of Au by a factor of about 3 following only 1–3 pulses. This result suggests a direction for future study of optical properties of nanostructures imprinted on a metal surface. Second, our study finds a type of microscale periodic structure with much finer nanoscale structures following ablation with a large number of applied pulses. This observation may

prompt us to reexamine our current understanding of the physical mechanism of periodic structure formation. Third, redeposition of laser-induced nanoparticles is also seen outside of the ablated spot leading to the formation of a nanostructured material known as gold black. Finally, our study also indicates potential applications of femtosecond laser ablation for modifying optical properties of metals and producing technologically valuable surface coatings such as gold-black films.

ACKNOWLEDGMENTS

The authors acknowledge J. Dai and B. McIntire for assistance with SEM micrographs. The research was supported by NSF and DARPA administered through ARO.

-
- ¹D. Perez and L. J. Lewis, *Phys. Rev. B* **67**, 184102 (2003).
²R. Stoian, A. Rosenfeld, D. Ashkenasi, I. V. Hertel, N. M. Bulgakova, and E. E. B. Campbell, *Phys. Rev. Lett.* **88**, 097603 (2002).
³F. Vidal, T. W. Johnston, S. Laville, O. Barthelemy, M. Chaker, B. Le Droff, J. Margot, and M. Sabsabi, *Phys. Rev. Lett.* **86**, 2573 (2001).
⁴B. N. Chichkov, C. Momma, S. Nolte, F. von Alvensleben, and A. Tunnermann, *Appl. Phys. A* **63**, 109 (1996).
⁵G. Ausanio, A. C. Barone, V. Iannotti, L. Lanotte, S. Amoruso, R. Bruzzese, and M. Vitiello, *Appl. Phys. Lett.* **85**, 4103 (2004).
⁶M. M. Murnane, H. C. Kapteyn, and R. W. Falcone, *Phys. Rev. Lett.* **62**, 155 (1989).
⁷S. Eliezer, N. Eliaz, E. Grossman, D. Fisher, I. Gouzman, Z. Henis, S. Pecker, Y. Horovitz, M. Fraenkel, S. Maman, and Y. Lereah, *Phys. Rev. B* **69**, 144119 (2004).
⁸S. Amoruso, G. Ausanio, R. Bruzzese, M. Vitiello, and X. Wang, *Phys. Rev. B* **71**, 033406 (2005).
⁹D. Scuderi, O. Albert, D. Moreau, P. P. Pronko, and J. Etchepare, *Appl. Phys. Lett.* **86**, 071502 (2005).
¹⁰A. Y. Vorobyev and Chunlei Guo, *Appl. Phys. Lett.* **86**, 011916 (2005).
¹¹J. M. Elson and C. C. Sung, *Appl. Opt.* **21**, 1496 (1982).
¹²M. Bass and L. Liou, *J. Appl. Phys.* **56**, 184 (1984).
¹³A. M. Prokhorov, V. I. Konov, I. Ursu, and I. N. Mihailescu, *Laser Heating of Metals* (Adam Hilger, Bristol, 1990).
¹⁴R. Fedosejevs, R. Ottmann, R. Sigel, G. Kühnle, S. Szatmari, and F. P. Schäfer, *Phys. Rev. Lett.* **64**, 1250 (1990).
¹⁵A. Ng, P. Celliers, A. Forsman, R. M. More, Y. T. Lee, F. Perrot, M. W. C. Dharmawardana, and G. A. Rinker, *Phys. Rev. Lett.* **72**, 3351 (1994).
¹⁶D. F. Price, R. M. More, R. S. Walling, G. Guethlein, R. L. Shepherd, R. E. Stewart, and W. E. White, *Phys. Rev. Lett.* **75**, 252 (1995).
¹⁷D. Fisher, M. Fraenkel, Z. Henis, E. Moshe, and S. Eliezer, *Phys. Rev. E* **65**, 016409 (2001).
¹⁸L. K. Ang, Y. Y. Lau, R. M. Gilgenbach, and H. L. Spindler, *Appl. Phys. Lett.* **70**, 696 (1997).
¹⁹U. Kreibig and M. Vollmer, *Optical Properties of Metal Clusters* (Springer-Verlag, Berlin, 1995).
²⁰C. G. Granqvist and O. Hunderi, *Phys. Rev. B* **16**, 3513 (1977).
²¹I. Ursu, I. N. Mihailescu, A. M. Prokhorov, V. I. Konov, and V. N. Tokarev, *Physica B & C* **132C**, 395 (1985).
²²W. Becker, R. Fetting, A. Gaymann, and W. Ruppel, *Status Solidi B* **194**, 241 (1996).
²³J. Lehman, E. Theocharous, G. Eppeldauer, and C. Pannell, *Meas. Sci. Technol.* **14**, 916 (2003).
²⁴D. J. Advena, V. T. Bly, and J. T. Cox, *Appl. Opt.* **32**, 1136 (1993).
²⁵W. Becker, R. Fetting, and W. Ruppel, *Infrared Phys. Technol.* **40**, 431 (1999).
²⁶D. M. Schaadt, B. Feng, and E. T. Yu, *Appl. Phys. Lett.* **86**, 063106 (2005).